International Journal of Metallurgical Engineering 2013, 2(1): 10-17
DOI: 10.5923/j.ijmee.20130201.02

Microstructural Simulations via Thermal Processing of Roll Bonded Steel Laminates

David K. Matlock*, Ralph J. Johnson, Emmanuel De Moor, John G. Speer

Advanced Steel Processing and Products Research Center , Colorado School of Mines, Golden, Cousa, 80401

Abstract Laboratory processed laminated composites, designed to simulate compositional gradients present in cast and hot rolled industrial microstructures, wereused to assess microstructural evolution during heat treating and the effects of specific microstructural variables on mechanical propertiesin steels. In this paper, two microstructural systems are presented to illustrate the broad applicability of the simulation technique. In one example, artificial compositional segregation of Mn was introduced to simulate microstructural banding observed in most industrial cast and hot rolled steels. Laminates were produced from two nominally 0.4 wtpct C steels with either 0.82 or 1.83 wtpctMn. The effects of composition band width and heat treatment, designed to alter the sharpness of the Mn gradients between layers, on microstructures andtensile properties are presented. In a second example, multiphase microstructures characteristic of the next generation advanced high strength sheet steels (AHSS) were simulated by roll bonding alternating layers of a steel with 2 wtpctMn and another steel with 18 wtpctMn. The resulting mechanical properties correlate to predictions of a composite model when sufficient interfacial strength was achieved to prevent tunnel crack formation.

Keywords Laminated Composites, AHSS, Simulated Microstructures, Banding

1. Introduction

Multi-scale modeling analyses which lead to property predictions of steel microstructures with multiple constituents (e.g. ferrite, bainite, martensite, austenite, carbide precipitates, inclusions, etc.) have become important components of research programs designed to identify, and eventually produce, new steels with enhanced properties for critical applications[1-4]. Essential to all models, are expressions that describe the deformation characteristics (yielding, strain hardening, etc.) of the individual constituents. The various modeling approaches differ with respect to the method used to integrate properties of individual phases and constituents and to incorporate interfacial properties and interactions between constituents. While most models concentrate on deformation behavior, some incorporate critical fracture criteria[5].

In steels with stable microstructures (i.e. without deformation induced transformation of austenite to martensite) interrelationships between microstructural constituents, strength, strain hardening, and ductility in tension are considered in terms of equations that relate operable strengthening mechanisms to strain-dependent expressions[1,2] and take the form shown in Eq. 1

$$\sigma(\varepsilon) = \sigma_i + \sigma_{SS} + \sigma_D + \sigma_{PPTN} + k_y d^{-1/2} \quad (1)$$

where $\sigma(\varepsilon)$ is the flow stress, σ_i is the friction stress of pure iron, σ_{SS} is the sum of solid solution strengthening contributions, σ_D is the strain-dependent strengthening from dislocation substructure, σ_{PPTN} is the contribution from precipitation hardening, ky is the Hall-Petch slope, and d is the grain diameter. Alternately, Ashby showed that for selected cases, the strength and strain hardening behavior of a multiphase material can be described by a “one-parameter” theory where strain-dependent strength depends only on the strain dependence of the average dislocation density, ρ_{AVG}[6].

Descriptions of constituent interactions primarily involve micromechanical models based on finite element analyses which incorporate predictions utilizing representative volume elements (RVE)[3,4,7] and composite models which describe modified rule-of-mixtures[1,2,8]. Both approaches recognize microstructural inhomogeneitiesand assess position-dependent variations in phases, constituents, and properties. In each case, experimental measurements are required to provide data to validate model predictions. Materials utilized in validation experiments may include commercially produced steels selected to assess microstructural variablesor specially processed model alloys designed and processed to produce controlled phase distributions. Production of roll bonded laminate composites, the subject of this paper, offers a unique method to produce model materials with systematically controlled

* Corresponding author:
dmatlock@mines.edu (David K. Matlock)
Published online at http://journal.sapub.org/ijmee

microstructural variables. The potential importance of layered materials has been recognized by the Ministry of Education, Culture, Sports, Science and Technology of Japan through funding of the multi-site Layer-Integrated Steels and Metals Project[9].

In this paper the procedure to produce roll bonded laminated composites is summarized and a brief review of selected studies of laboratory-produced materials designed to evaluate specific variables in non-uniform microstructure sis presented[10-13]. This background information provides the basis for a study to physically simulate microstructural variables in potential 3rd generation advanced high strength steels (AHSS) and evaluate predictions of a composite model that has provided insight into new AHSS microstructures [1,2].

2. Laboratory Production of Simulated Microstructures

A roll bonding procedure was developedto processa variety of alloy combinations on a laboratory rolling mill with 133 mm diameter by 203 mm face work rolls[10-13]. Typically two component materials were evaluated; the procedure could be easily modified toincorporate more than two primary constituents. Prior to fabrication of the final roll bonded compact, each experimental material was hot rolled, and in some cases cold rolled, to a final thickness of nominally 0.5 mm. To facilitate bonding and to eliminate the presence of undesirable inclusions at bond interfaces, prior to roll bonding, all sheet surfaces were pickled to remove oxides and mechanically cleaned with a commercial abrasive cloth.

Figure 1 shows the procedure for fabricating the roll bonded laminated compacts. For each two-component material of interest,alternating sheet layers, nominally 0.5 mm thick with widths and lengths of 90 and 125 mm, respectively, were encased in a welded stainless steel box. Figure 2 shows an example welded compact that included a vacuum attachment tube welded to one end. During TIG welding the layered stack and formed stainless steel box parts were compressed in a hydraulic press to minimize space between layers. The relative volume fractions of each constituent were varied by controlling sheet thickness.

The welded boxes were connected to an active vacuum system and preheated to the desired rolling temperature selected based on the specific alloys of interest. The compacts were hot rolled to the final sheet thicknesses selected to produce specific band thicknesses based on the initial sheet thicknesses of the individual layers. To ensure bonding, the initial pass was the maximum achievable on the laboratory rolling mill. Typically primary bonding occurred in the first one or two passes and after three to four passes the vacuumtube separated fromthe compact. Subsequent rolling was completed in air, and intermediate reheating was used as necessary.

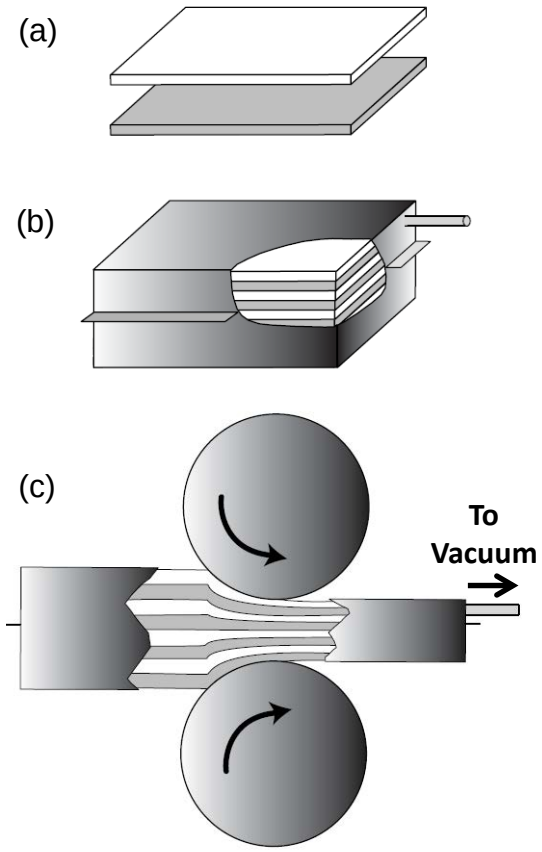

Figure 1. Schematic of production steps for roll bonded laminated composites (a) alternately stacked sheets; (b) sheet compacts sealed in stainless steel boxes; and (c) boxes attached to an active vacuum system and hot rolled[13]

Figure 2. Example TIG welded stainless steel box prior to hot rolling[12]

3. Review of Model Systems

Roll bonded laminate composites have been used to model properties in steels and other alloys with multi-component microstructures and have been used to produce new materials with enhanced properties[14,15]. Selected example systems and fundamental principles that have been considered include the following: fabrication and properties of Damascus steels[14]; fabrication and fracture assessment of high energy absorbing materials[16,17]; alloy

homogenization during annealing with results applicable to cored castings and weldmentsand the effects of cored microstructures on the high temperature mechanical properties of weldments[18,19]; homogenization of thin thermally-sprayed coatings on substrates at elevated temperatures[20]; neutron diffraction studies of stress partitioning during deformation of multi-phase steels[21]; fundamental analyses of the Kirkendall effect and diffusion-induced porosity formation[22]; and banding in steels[11-13].In the latter studies, manganese banding and its potential effects on phase transformations and heat treat responses of steels were considered and selected results are presented here.

Banded 0.4 C steels with alternating equal-thickness layers of 0.8 or 1.8 Mn (wtpct) were processed with band widths between 10 and 320 μm to simulate banding observed in rolled and/or forged SAE 5140 steel and used to evaluate the effects of band width on phase transformations and tensile properties[11-13]. Results assessed the effects of heating and of cooling rates (83°C/s to $8.3x10^{-3}$°C/s) on phase transformations and layer interactions critical to the development of the final microstructures. To illustrate the importance of banding on layer-dependent properties, Fig. 3 shows engineering stress-strain curves for samples with various band widths cooled at 0.6°C/s (Fig. 3a) and $1.7x10^{-2}$°C/s (Fig. 3b) from 850°C[11]. The tensile properties for samples cooled at 0.6°C/s depend sensitively on band width, which, as discussed below, reflects the development of diffusion controlled interfacial layers of constant thickness. In contrast, the properties for samples cooled at a much lower rate (Fig. 3b) are essentially independent of band thickness.

The cooling-rate dependence of the effects of layer thickness were clarified via light optical microstructure analyses[11,12] and selected micrographs for samples cooled at 0.6°C /s from 850°C are shown in Figs. 4a and 4b for 160 and 20 μm samples, respectively. At this intermediate cooling rate, a 20 μm interfacial band of pearlite[12] developed in addition to the ferrite pearlite band in the low Mn layer and a high strength bainitic band in the high Mn layer. In contrast, the pearlitic interface band is shown to completely encompass the high Mn layer in the 20 μm thick banded condition. Thus, with an increase in layer thickness, the volume fraction of the high strength bainitic band increases with band width leading to the strength effects shown in Fig. 3a. At the lower cooling rate ($1.7x10^{-2}$°C/s), alternating ferrite-pearlite bands developed and the tensile properties were independent of band width (Fig. 3b). Related studies have shown that as a result of composition gradients in banded steels, displacements associated with the differential transformation response between layers and response to non-uniform heating, as imposed during induction hardening, depend on orientation with respect to the banded structure[12,23].

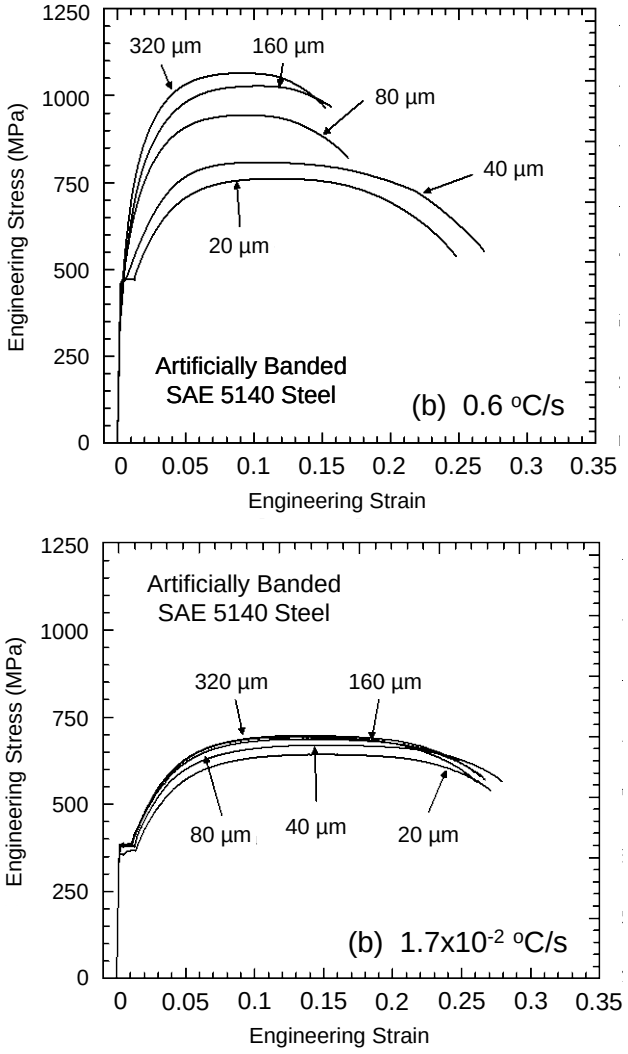

Figure 3. Room temperature engineering stress strain curves for artificially banded SAE 5140 steel processed with band widths between 20 and 320 μm and cooled at (a) 0.6 °C/s and (b) $1.7x10^{-2}$°C/s[11]

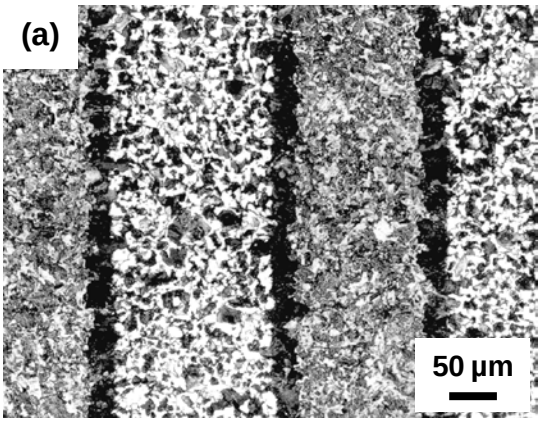

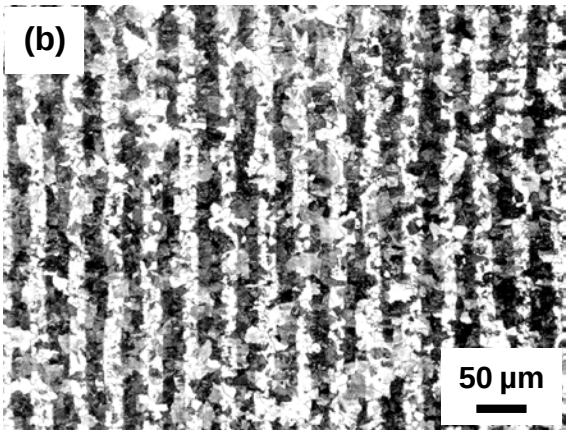

Figure 4. Light optical micrographs of artificially banded SAE 5140 steel cooled at 0.6 °C/s with band widths of (a) 160 µm and (b) 20 µm (2 pctnital etch)[11]

4. Third Generation Advanced High Strength Steels (Ahss)

Recently there has been considerable interest to develop and evaluate models to predict properties characteristic of the new class of sheet steels referred to as the "Third Generation of Advanced High Strength Steels (AHSS)"[24,25]. One approach, based on the application of a multi-component iso-strain composite model[1,2,26] to multi-phase steels, has provided insight into microstructural constituents that will be required for Third Generation AHSS products. Predictions of tensile instability (i.e. combinations of uniform elongation and ultimate tensile strength) based on assumed mixtures of ferrite + martensite or (stable) austenite + martensite are overlaid in Fig. 5 on a property map developed by AISI[24]. The property comparisons show that mixtures of ferrite and higher strength martensite (or "ultra-fine" ferrite) are attractive and represent a broad range of ferrite-based steels while austenite + martensite combinations generate properties well within the targeted Third Generation property band.

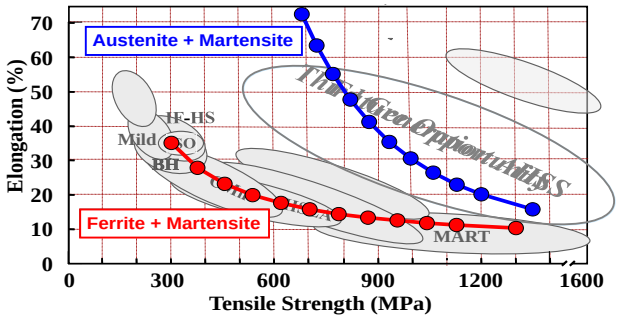

Figure 5. Tensile elongation/strength combinations for various steel families and 3rd Generation AHSS overlaid with property combinations predicted for various combinations of martensite and ferrite or (stable) austenite[1]

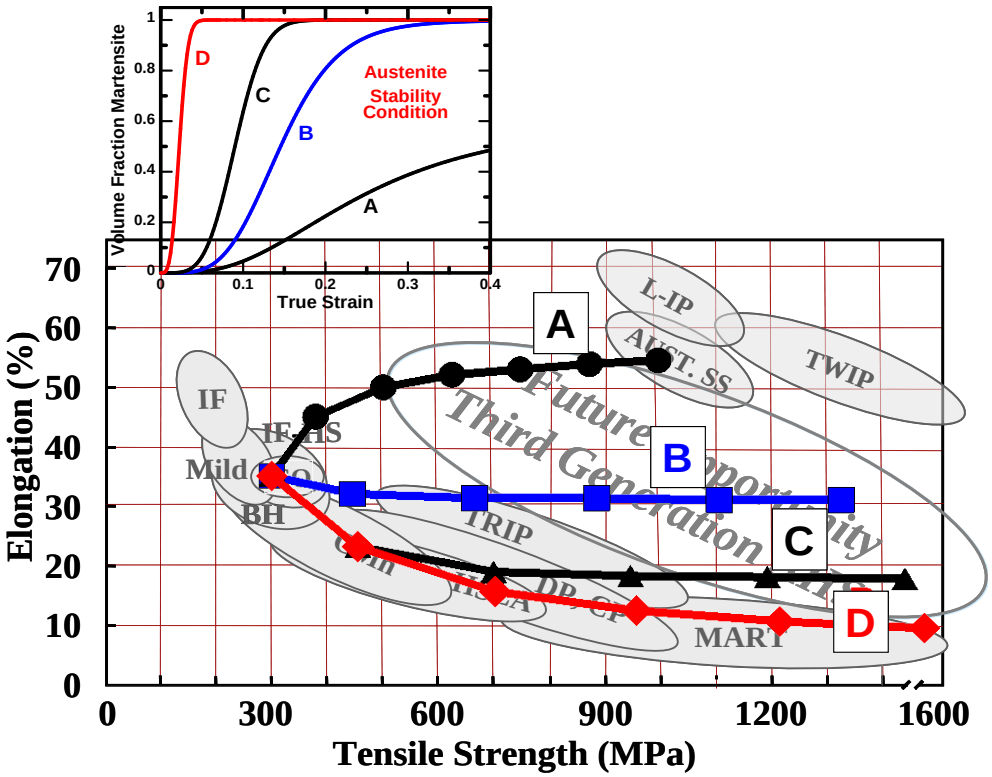

Figure 6. Tensile ductility/strength combinations for mixtures of martensite and metastable austenite, with austenite mechanical stability varying as shown in inset[2]

The composite analysis shows significant volume fractions of austenite, having a high capacity for work hardening, are probably necessary for the next-generation AHSS grades. The importance of austenite stability was also predicted with the composite modeling approach[2] and Fig. 6 illustrates predicted uniform elongation/tensile strength combinations for ferrite +austenite mixtures, where the mechanical stability of the austenite is varied according to the hypothetical behaviors shown in the inset. This analysis highlights the importance of controlling austenite stability as the very unstable material D exhibits properties essentially equivalent to the ferrite + martensite materials shown in Fig. 5, whereas the greater stability in material A provides exceptional property combinations.

To further understand the applicability of the simple composite model used to develop the predictions in Figs. 5 and 6, the following study to assess alternating roll-bonded layers of a stable austenitic steel and a dual-phase ferritic steel, in which the volume fractions of martensite were systematically varied by heat treatment, was undertaken. Roll bonded laminate composites consisting of equal thickness layers of a Twinning Induced Plasticity (TWIP) steel (18-Mn: in wtpct - 0.6C, 18Mn, 0.31Si, 0.38Cr, 0.04Nb, 0.04V, 1.5Al, 0.046S, 0.16P) and a dual-phase steel grade (2-Mn:in wtpct - 0.08C, 2.04Mn, 0.03Si, 0.27Cr, 0.28Mo, 0.06Al,0.01N, 0.01S, 0.02P) were hot rolled to 1.3 mm. Sub-sized ASTM E8 tensile samples were machined transverse to the rolling direction and contained a reduced gage section of 25 mm by 6 mm. These samples were then annealed in salt pots at 685°C, 730°C, 790°C, and 865°C for 10 min and immediately water quenched. Temperatures were selected to produce systematic variations in the volume fraction of martensite in the dual-phase steel layers as summarized in Table 1.A minimum of three tensile tests for each heat treat condition was performed at room temperature with an imposed engineering strain rate of 3.4×10^{-4}.

Table 1. Constituent fractions for annealed and quenched samples

Phase	Volume Fractions for Annealed Samples			
	685°C	730°C	790°C	865°C
Austenite	0.5	0.5	0.5	0.5
Ferrite	0.3	0.2	0	0
Martensite	0.2	0.3	0.5	0.5

Table 2 summarizes the assumed constituent properties incorporated in a simple Hollomon power-law equation relating stress to plastic strain[1] used in the model predictions discussed below. The parameters for ferrite and martensite represent typical properties within the property bands shown in Figs. 5 and 6[1]. The mechanical properties for the austenite were obtained from tensile tests performed on the as received hot rolled 18-Mn sheet[27].

Figure 7 shows micrographs for the as-rolled composite (Fig. 7a) and after annealing at 685°C, 730°C, and 790°C. For the hot rolled condition, Fig. 6a shows a thin diffusional mixing region between the 18-Mn and 2-Mn layers as well as a darker ferritic based microstructure in the 2 Mn layer. Samples annealed at 685°C (Fig. 6b) and 730°C (Fig. 6c) contain four thin dark bands of martensite, and layers of ferrite in the 2-Mn layers. Figure 1d, for the sample annealed at 790°C indicates that the 2-Mn layer was fully martensitic, and the same is true for the sample annealed at 865°C, not shown here. It should be noted that due to the significant compositional differences some etching artifacts (e.g. dark spots) were apparent but assumed to not represent significant microstructural constituents.

Table 2. Model parameters for composite analysis

Phase	UTS (MPa)	Uniform True Strain
Austenite	1000	0.55
Ferrite	300	0.3
Martensite	1600	0.08

Figure 8 shows representative engineering stress strain curves for each heat treated sample. With an increase in annealing temperature the volume fraction of martensite increased leading to the observed increase in strength and decrease in ductility. The sample annealed at 685 °C was the only sample to exhibit significant post uniform strain. To correlate with predictions based on the simplified composite model leading to the predictions in Fig. 5, the constituent parameters in Table 2 were used along with phase fractions based on light optical microscopy of deformed microstructures and calculated by measured line lengths through the thickness for each phase.

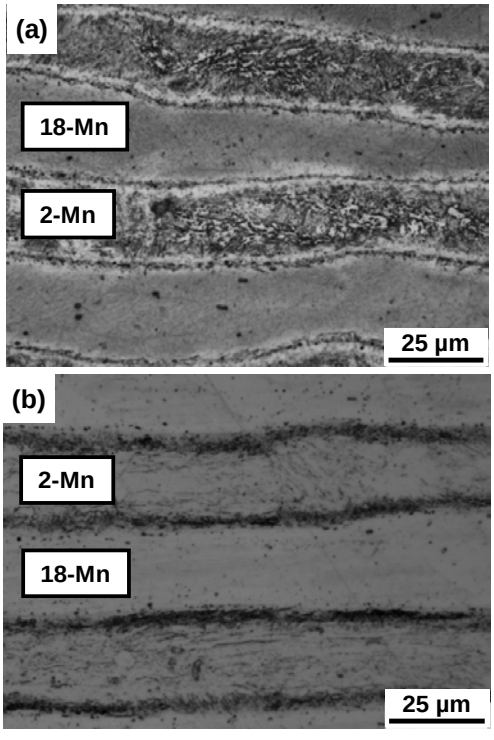

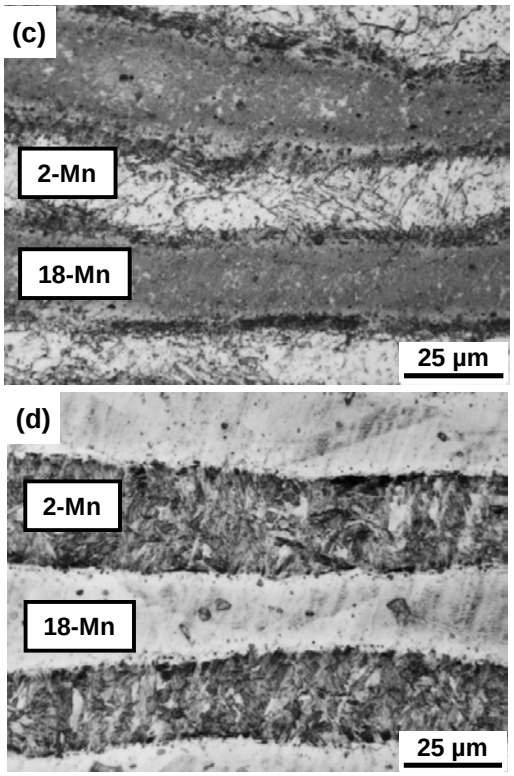

Figure 7. Light optical micrographs of the 2-Mn/18-Mn laminate composite in the (a) as hot rolled condition or after annealing at (b) 685°C, (c) 730°C, and (d) 790°C (etched with 10 pctnital)

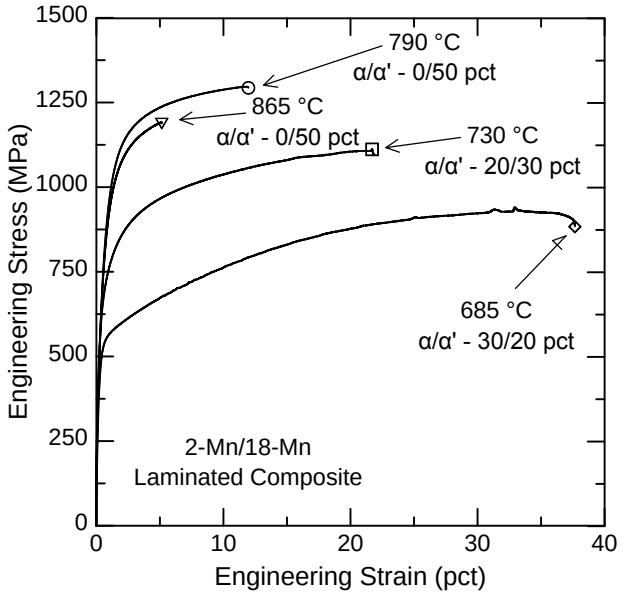

Figure 8. Representative engineering stress-strain curves for the 2-Mn/18-Mn laminate composite after quenching from the indicated temperatures

Figure 9 compares modeled and actual tensile data. For reference, the solid line represents composites consisting of ferrite (α) and martensite (α') and the dashed line represents composites of three phases consisting of 50 percent austenite (γ), and systematically varied ferrite (α) and martensite (α') contents. For the calculations here, the effects of martensite carbon content on martensite properties were not considered but could be incorporated in future studies. The mechanical properties predicted by the model are plotted as solid symbols for each annealing condition. The open symbols are the experimentally measured values. The samples annealed at 685 °C and 730 °C exhibit good agreement with the model, however the samples annealed at higher temperatures exhibit ductilities significantly less than predicted.

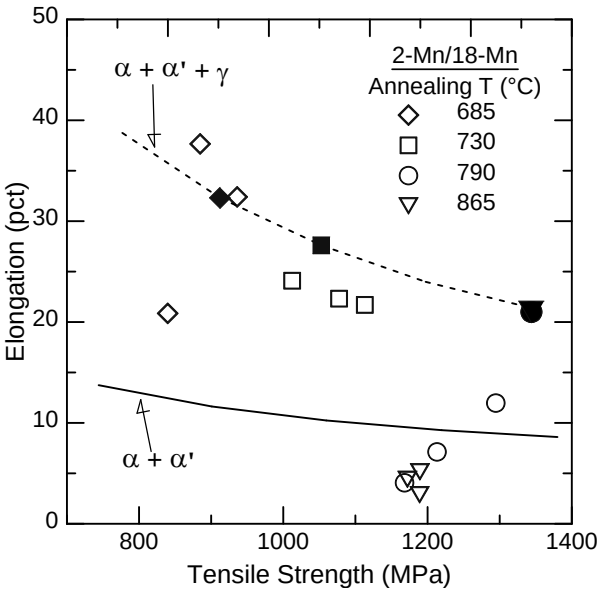

Figure 9. A comparison of the predictions (closed symbols) for the 2-Mn/18-Mn laminate composite model analysis with experimentally measured tensile properties (open symbols)

To resolve the discrepancies observed between measured and predicted properties for the samples annealed at the two higher temperatures, the fracture behavior of each sample was evaluated with light optical microscopy of cross sections of failedsamples. Figure 10 shows micrographs for samples annealed at 730 °C and 790 °C, which arealso representative of the behavior of samples annealed at 685 °C and 865 °C, respectively. Samples annealed at the lower temperatures (e.g. Fig. 10a) exhibited ductile fracture of both layers and sufficient plasticity in the interfacial martensite layer to maintain cohesion between layers. In contrast, Fig. 10b shows that for the higher annealing temperatures the martensitic 2-Mn layers failed in a brittle manner without localized necking and with significant interfacial crack formation. As a consequence of the brittle fracture, a critical assumption of the simplified isostraincomposite model, i.e. continuous bonding leading to enhanced ductility of the high strength layers[1,26], was not met. As a result, the measured ductilities for samples annealed at the two higher temperatures were less than predicted. It was also interpreted that with an increase in the volume fraction of martensite, in the presence of the P added to the 18-Mn steel, P diffusion to the interface may have decreased the critical stress required to grow tunnel cracks[28], further decreasing the laminate ductility by removing constraint on the high strength martensitic layers. This study illustrates that the laminated composite model[1,2] successfully predicts third generation AHSS tensile properties for those conditions where interfacial fracture was suppressed.

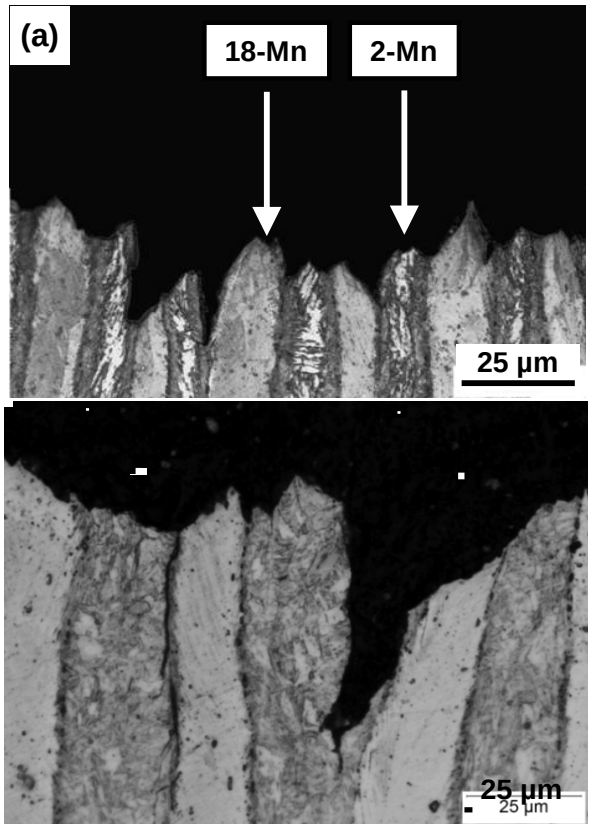

Figure 10. Light optical micrographs of fractured tensile samples of 2-Mn/18-Mn laminate quenched from (a) 730°C and (b) 790°C

5. Summary

A laboratory technique to produce simulated complex microstructures with roll bonded laminated composites has been shown to provide a unique method for evaluating the effects of heat treating on microstructures and properties of multi-phase steel alloys. Insight provided by the simple composite model analysis which successfully predicted tensile properties in a microstructural system designed to simulate potential Third Generation AHSS products provides guidance for the development of future AHSS microstructures and properties. The results also illustrate the potential importance of interdiffusion between layers on microstructure development.

ACKNOWLEDGEMENTS

The authors gratefully acknowledge the support of the National Science Foundation for support under award CMMI-0729114 and the sponsors of the Advanced Steel Processing and ProductsResearchCenter, an industry/university cooperative research center at the Colorado School of Mines.

REFERENCES

[1] D.K. Matlock and J.G. Speer, Proc. of the 3rd Int. Conf. Structural Steels, Ed. H.C. Lee, The Korean Institute of Metals and Materials, Seoul, Korea, 2006, pp. 774-781.

[2] D.K. Matlock and J.G. Speer, Microstructure and Texture in Steels and Other Materials, Ed. A. Haldar, S. Suwas, and D. Bhattacharjee, Springer, London, 2009, pp. 185-205.

[3] K.S. Choi, W. Liu, X. Sun, and M.A. Khaleel, Metall. and Mat. Trans. A, Vol. 40, No. 4, 2009, pp. 796-809.

[4] C. Krempaszky, E. Werner, T. Hebesberger and A. Pichler, Proc.Int. Conf. on New Developments in Advanced High-Strength Sheet Steels, Ed. J.G. Speer, B. Nelson, and R. Pradhan, AIST, Warrendale, PA, 2008, pp. 305-314.

[5] F.J. Franklin, J.E. Garnham, D.I. Fletcher, C.L. Davis, A. Kapoora, Wear, Vol. 265, 2008, pp. 1332-1341.

[6] M.F. Ashby, Strengthening Methods in Crystals, Ed A. Kelly and R.B. Nicholson, Elsevier Pub., Amsterdam, 1971, pp. 137-192.

[7] K.S. Choi, A. Soulami, W.N. Liu, X. Sun. M.A. Khaleel, Computational Mat. Sci., Vol. 50, 2010, pp. 720–730.

[8] R.G. Davies, Metall. Trans. A, Vol. 9A, 1978, pp. 41-52.

[9] S. Nambu, M. Michiuchi, Y. Ishimoto, K. Asakura, J. Inoue, and T. Koseki, Scripta Mat., Vol. 60, 2009, pp. 221-224.

[10] I.D. Choi, D.K. Matlock, and D.L. Olson, Metall. Trans. A, Vol. 21A, 1990, pp. 2513-2520.

[11] T.F. Majka, D.K. Matlock, G. Krauss, and M.T. Lusk, Proc. of the 42nd Mech. Working and Steel Proc. Conf., October 2000, ISS AIME, Warrendale, PA, 2000, pp. 75-87.

[12] T.F. Majka, D.K. Matlock, G. Krauss, Metall. and Mat. Trans., Vol. 33A, 2002, pp. 1627-1637.

[13] R.A. Jaramillo, M.T. Lusk, and M.C. Mataya, Acta Mat., Vol. 52, 2004, pp. 851-858.

[14] D. R. Lesuer, C. K. Syn, O. D. Sherby, J. Wadsworth, J. J. Lewandowski, and W. H. Hunt, Jr, ," Int. Mat. Rev., Vol. 41, 1966, pp. 169-197.

[15] S. Nambu, M. Michiuchi, J. Inoue, and T. Koseki, Comp. Sci. and Tech., Vol. 69, 2009, pp. 1939-1941.

[16] F. Carreño, J. Chao, M. Pozuelo, O.A. Ruano, Scripta Mat., Vol. 48, 2003, pp. 1135-1140.

[17] C.K. Syn, D.R. Lesuer, J. Wolfenstine, and O.D. Sherby, Metall. Trans. A, Vol. 24A, 1993, pp. 1647-1653.

[18] I.D. Choi, D.K. Matlock, and D.L. Olson, Recent Trends in Welding Sci.e and Tech., Ed. by S.A. David and J.M. Vitek, ASM, Metals Park, OH, 1990, pp. 787 791.

[19] S.H. Wang, D.K. Matlock, and D.L. Olson, ScriptaMet.and Mat., Vol. 27, 1992, pp. 35-40.

[20] B. Klusemann and B. Svendsen, Int. J. of Solids and Structures, Vol. 49, 2012, pp. 1828–1838.

[21] M. Ojima, J. Inoue, S. Nambu, P. Xu, K. Akita, H. Suzuki, and T. Koseki, Scripta Mat., Vol. 66, 2012, pp. 139-142.

[22] I.D. Choi, D.K. Matlock, and D.L. Olson, Mat. Sci. and Engr., Vol. A124, 1990, pp. L15-L18.

[23] P.I. Anderson, D.K. Matlock and J.G. Speer, Proc. of Int. Conf. on New Dev. in Long and Forged Products: Metallurgy and Applications, Ed. J.G. Speer, E.B. Damm and C.V. Darragh, AIST, Warrendale, PA, USA, 2006, pp. 107-116.

[24] "Third Generation Advanced High Strength Steel (AHSS)," Research and Development Solicitation, AISI, Washington, DC, 2006.

[25] E. De Moor, P. J. Gibbs, J. G. Speer, D.K. Matlock, and J.G. Schroth, AIST Trans., Iron & Steel Tech., Vol. 7, No. 11, 2010, pp. 133-144.

[26] S.T Mileiko, J. of Mat. Sci., Vol. 4, 1969, pp. 974-977.

[27] J.A. Ronevich, J.G. Speer, and D.K. Matlock, SAE Int. J. Mater. Manuf., vol. 3, no. 1, 2010, pp. 255-267.

[28] S. Ho and Z. Suo, Trans. of the ASME, Vol. 60, 1993, pp. 890-894.